DOI:10.1158/1535-7163.MCT-10-0544

and growth is cell density-dependent in HepG2 cells. J Cell Physiol 2007;210:766–73.
12. Mizuguchi T, Nagayama M, Meguro M, et al. Prognostic impact of surgical complications and preoperative serum hepatocyte growth factor in hepatocellular carcinoma patients after initial hepatectomy. J Gastrointest Surg 2009;13:325–33.
13. Chau GY, Lui WY, Chi CW, et al. Significance of serum hepatocyte growth factor levels in patients with hepatocellular carcinoma undergoing hepatic resection. Eur J Surg Oncol 2008;34:333–8.
14. Yamagamim H, Moriyama M, Matsumura H, et al. Serum concentrations of human hepatocyte growth factor is a useful indicator for predicting the occurrence of hepatocellular carcinomas in C-viral chronic liver diseases. Cancer 2002;95:824–34.
15. Tanaka K, Arao T, Maegawa M, et al. SRPX2 is overexpressed in gastric cancer and promotes cellular migration and adhesion. Int J Cancer 2009;124:1072–80.
16. Matsumoto K, Arao T, Tanaka K, et al. mTOR signal and hypoxia-inducible factor-1 alpha regulate CD133 expression in cancer cells. Cancer Res 2009;69:7160–4.
17. Kaneda H, Arao T, Tanaka K, et al. FOXQ1 is overexpressed in colorectal cancer and enhances tumorigenicity and tumor growth. Cancer Res 2010;70:2053–63.
18. Lee JM, Dedhar S, Kalluri R, Thompson EW: The epithelial-mesenchymal transition: new insights in signaling, development, and disease. J Cell Biol 2006;172:973–81.
19. Wheelock MJ, Shintani Y, Maeda M, Fukumoto Y, Johnson KR. Cadherin switching. J Cell Sci 2008;121:727–35.
20. Lo HW, Hsu SC, Xia W, et al. Epidermal growth factor receptor cooperates with signal transducer and activator of transcription 3 to induce epithelial-mesenchymal transition in cancer cells via up-regulation of TWIST gene expression. Cancer Res 2007;67:9066–76.
21. Vincent T, Neve EP, Johnson JR, et al. A SNAIL1-SMAD3/4 transcriptional repressor complex promotes TGF-beta mediated epithelial-mesenchymal transition. Nat Cell Biol 2009;11:943–50.
22. Larue L, Bellacosa A. Epithelial-mesenchymal transition in development and cancer: role of phosphatidylinositol 3' kinase/AKT pathways. Oncogene 2005;24:7443–54.
23. Zavadil J, Böttinger EP. TGF-beta and epithelial-to-mesenchymal transitions. Oncogene 2005;24:5764–74.
24. Liu L, Cao Y, Chen C, et al. Sorafenib blocks the RAF/MEK/ERK pathway, inhibits tumor angiogenesis, and induces tumor cell apoptosis in hepatocellular carcinoma model PLC/PRF/5. Cancer Res 2006;66:11851–8.
25. Voulgari A, Pintzas A. Epithelial-mesenchymal transition in cancer metastasis: mechanisms, markers and strategies to overcome drug resistance in the clinic. Biochim Biophys Acta 2009;1796:75–90.
26. Yauch RL, Januario T, Eberhard DA, et al. Epithelial versus mesenchymal phenotype determines *in vitro* sensitivity and predicts clinical activity of erlotinib in lung cancer patients. Clin Cancer Res 2005; 11:8686–98.
27. Thomson S, Petti F, Sujka-Kwok I, Epstein D, Haley JD. Kinase switching in mesenchymal-like non-small cell lung cancer lines contributes to EGFR inhibitor resistance through pathway redundancy. Clin Exp Metastasis 2008;25:843–54.
28. Fuchs BC, Fujii T, Dorfman JD, et al. Epithelial-to-mesenchymal transition and integrin-linked kinase mediate sensitivity to epidermal growth factor receptor inhibition in human hepatoma cells. Cancer Res 2008;68:2391–9.
29. Arumugam T, Ramachandran V, Fournier KF, et al. Epithelial to mesenchymal transition contributes to drug resistance in pancreatic cancer. Cancer Res 2009;69:5820–8.
30. Wang Z, Li Y, Kong D, et al. Acquisition of epithelial-mesenchymal transition phenotype of gemcitabine-resistant pancreatic cancer cells is linked with activation of the notch signaling pathway. Cancer Res 2009;69:2400–7.
31. Kudo-Saito C, Shirako H, Takeuchi T, Kawakami Y. Cancer metastasis is accelerated through immunosuppression during Snail-induced EMT of cancer cells. Cancer Cell 2009;15:195–206.
32. von Burstin J, Eser S, Paul MC, et al. E-cadherin regulates metastasis of pancreatic cancer *in vivo* and is suppressed by a SNAIL/HDAC1/HDAC2 repressor complex. Gastroenterology 2009;137:361–71.
33. Yang MH, Chen CL, Chau GY, et al. Comprehensive analysis of the independent effect of Twist and Snail in promoting metastasis of hepatocellular carcinoma. Hepatology 2009;50:1464–74.

Published OnlineFirst December 3, 2010; DOI:10.1158/1078-0432.CCR-09-2755

Clinical Cancer Research

Antitumor Activity of BIBF 1120, a Triple Angiokinase Inhibitor, and Use of VEGFR2 $^{+}$pTyr^{+} Peripheral Blood Leukocytes as a Pharmacodynamic Biomarker *In Vivo*

Kanae Kudo, Tokuzo Arao, Kaoru Tanaka, et al.

Clin Cancer Res 2011;17:1373-1381. Published OnlineFirst December 3, 2010.

Published OnlineFirst December 3, 2010; DOI:10.1158/1078-0432.CCR-09-2755

Clinical Cancer Research

Cancer Therapy: Preclinical

Antitumor Activity of BIBF 1120, a Triple Angiokinase Inhibitor, and Use of VEGFR2$^+$pTyr$^+$ Peripheral Blood Leukocytes as a Pharmacodynamic Biomarker *In Vivo*

Kanae Kudo[1,2], Tokuzo Arao[1], Kaoru Tanaka[1], Tomoyuki Nagai[1], Kazuyuki Furuta[1], Kazuko Sakai[1], Hiroyasu Kaneda[1], Kazuko Matsumoto[1], Daisuke Tamura[1], Keiichi Aomatsu[1], Marco A. De Velasco[1], Yoshihiko Fujita[1], Nagahiro Saijo[3], Masatoshi Kudo[2], and Kazuto Nishio[1]

Abstract

Purpose: BIBF 1120 is a potent, orally available triple angiokinase inhibitor that inhibits VEGF receptors (VEGFR) 1, 2, and 3, fibroblast growth factor receptors, and platelet-derived growth factor receptors. This study examined the antitumor effects of BIBF 1120 on hepatocellular carcinoma (HCC) and attempted to identify a pharmacodynamic biomarker for use in early clinical trials.

Experimental Design: We evaluated the antitumor and antiangiogenic effects of BIBF 1120 against HCC cell line both *in vitro* and *in vivo*. For the pharmacodynamic study, the phosphorylation levels of VEGFR2 in VEGF-stimulated peripheral blood leukocytes (PBL) were evaluated in mice inoculated with HCC cells and treated with BIBF 1120.

Results: BIBF 1120 (0.01 μmol/L) clearly inhibited the VEGFR2 signaling *in vitro*. The direct growth inhibitory effects of BIBF 1120 on four HCC cell lines were relatively mild *in vitro* (IC_{50} values: 2–5 μmol/L); however, the oral administration of BIBF 1120 (50 or 100 mg/kg/d) significantly inhibited the tumor growth and angiogenesis in a HepG2 xenograft model. A flow cytometric analysis revealed that BIBF 1120 significantly decreased the phosphotyrosine (pTyr) levels of VEGFR2$^+$CD45^{dim} PBLs and the percentage of VEGFR2$^+$pTyr$^+$ PBLs *in vivo*; the latter parameter seemed to be a more feasible pharmacodynamic biomarker.

Conclusions: We found that BIBF 1120 exhibited potent antitumor and antiangiogenic activity against HCC and identified VEGFR2$^+$pTyr$^+$ PBLs as a feasible and noninvasive pharmacodynamic biomarker *in vivo*. *Clin Cancer Res; 17(6); 1373–81. ©2010 AACR.*

Introduction

A number of antiangiogenic inhibitors have been studied in clinical settings, some of which have clearly exhibited a clinical benefit in oncology. Consequently, VEGFs and VEGF receptors (VEGFR) are now well-validated targets in cancer therapy (1). In hepatocellular carcinoma (HCC), 2 recent randomized controlled trials for HCC have reported a clinical benefit of single-agent sorafenib for extending the overall survival in both Western and Asian patients with advanced unresectable HCC (2, 3). On the basis of the clear results of these trials, sorafenib is presently regarded as the standard therapy for HCC.

Authors' Affiliations: Departments of [1]Genome Biology and [2]Gastroenterology, [3]Kinki University School of Medicine, Osaka, Japan

Note: Supplementary data for this article are available at Clinical Cancer Research Online (http://clincancerres.aacrjournals.org/).

Corresponding Author: Kazuto Nishio, Department of Genome Biology, Kinki University School of Medicine, 377-2 Ohno-higashi, Osaka-Sayama, Osaka 589-8511, Japan. Phone: 81-72-366-0221; Fax: 81-72-366-0206. E-mail: knishio@med.kindai.ac.jp

doi: 10.1158/1078-0432.CCR-09-2755

Because antiangiogenic inhibitors may achieve therapeutic levels long before toxicities arise compared with conventional cytotoxic chemotherapies, identifying pharmacodynamic biomarkers that accurately reflect the effects of the drug on its known targets are needed (4, 5). Therefore, a wide variety of biomarkers of antiangiogenic inhibitors have been proposed and intensively investigated, including plasma proteins, angiogenesis-related signaling, immunohistochemistry of endothelial cell markers for evaluating microvessel density (MVD), circulating endothelial progenitor/cells, and functional imaging such as dynamic contrast-enhanced MRI and molecular imaging using positron emission tomography (6). These candidate biomarkers have been evaluated and characterized as prognostic, pharmacodynamic, or response-predictive markers. Although the utility of biomarkers for evaluating MVD was highly anticipated, these markers were not predictive for clinical response in patients treated with bevacizumab (7). Regarding growth factors and cytokines, the plasma VEGF level has been shown to be neither a pharmacodynamic nor a predictive biomarker of antiangiogenic drugs (7, 8), although the plasma VEGF level is a well-known prognostic biomarker (9–11). Plasma-soluble VEGFR2, on the other hand, may be a promising and specific biomarker of

Published OnlineFirst December 3, 2010; DOI:10.1158/1078-0432.CCR-09-2755

Translational Relevance

A wide variety of biomarkers of antiangiogenic inhibitors have been proposed and intensively investigated; however, no biomarkers have been validated for routine clinical use and a new pharmacodynamic biomarker is needed. We have shown in this study that (i) BIBF 1120, a VEGF receptor 2 (VEGFR2) inhibitor, exhibited potent antitumor and antiangiogenic activity against hepatocellular carcinoma *in vivo* and (ii) $VEGFR2^{+}pTyr^{+}$ peripheral blood leukocytes (PBL) were useful pharmacodynamic biomarker *in vivo*. Our findings indicate the clinical utility of $VEGFR2^{+}pTyr^{+}$ PBLs as a feasible, noninvasive, and VEGF signal-specific biomarker of VEGFR2 tyrosine kinase inhibitors for use in early clinical trials.

antiangiogenic drugs for evaluating their effects (12, 13). Indeed, we have shown that soluble VEGFR2 was certainly decreased by BIBF 1120 treatment in a phase I trial; however, this decrease was observed at a relatively late stage, 8 to 29 days after the start of treatment (14). These results suggest that soluble VEGFR2 is not a rapid-responding biomarker for monitoring effects of antiangiogenic drugs. As no other biomarkers have been validated for routine clinical use, a new pharmacodynamic biomarker is needed.

BIBF 1120 is a potent triple angiokinase inhibitor that inhibits VEGFR1, 2, and 3, fibroblast growth factor receptors (FGFR), and platelet-derived growth factor receptors (PDGFR). *In vitro* studies have shown that VEGFR2 tyrosine kinase activity was potently inhibited by BIBF 1120 (IC_{50} = 21 nmol/L) and was also active against VEGFR1 and 3 (IC_{50} = 34 and 13 nmol/L, respectively; ref. 15). BIBF 1120 dose dependently inhibited the growth of various human tumor xenografts and tumor angiogenesis *in vivo* studies, consistent with the potent inhibition of VEGF signaling (15). BIBF 1120 also exhibited a relatively strong direct growth inhibitory effect on cancer cell lines, influencing 9 of 14 acute myeloid leukemia cell lines in a colony formation assay with an IC_{50} value of less than 1 μmol/L (16).

We previously reported the antitumor activity of VEGFR2 tyrosine kinase inhibitors (TKI) against non–small cell lung cancer and gastric cancer, identifying a biomarker and the mode of action (17–19). In the present study, we focused on the antitumor activity of BIBF 1120 against HCC, which is hypervascular in nature. In addition, to identify a pharmacodynamic biomarker, we examined the phosphorylation levels of VEGFR-positive peripheral blood leukocytes (PBL) as a surrogate tissue in an *in vivo* model.

Materials and Methods

Compounds

BIBF 1120 was provided by Boehringer Ingelheim Pharma GmbH & KG. 5-Fluorouracil (5FU; Sigma-Aldrich) and an epidermal growth factor receptor (EGFR) TKI, AG1478 (Biomol International), were purchased from the indicated companies.

Cell lines and cultures

HepG2, HLF, HLE, and Huh7 (human hepatoblastoma and HCC cell lines, respectively) were maintained in Dulbecco's modified Eagle's medium supplemented with 10% FBS (Gibco BRL). HUVECs (human umbilical vein endothelial cells) were purchased from Kurabo and were maintained in Humedia-EG2 (Kurabo) medium with 2% FBS, 2 ng/mL of VEGF-A (R&D Systems), 10 ng/mL of EGF, 5 ng/mL of FGF, 10 μg/mL of heparin, and 1 μg/mL of cortisol. These cells were cultured in an atmosphere of 5% CO_2 at 37°C.

In vitro growth inhibition assay

The growth inhibitory effects of BIBF 1120 on the HepG2, HLF, HLE, and Huh7 cell lines were examined using an MTT assay as previously described (17, 18). The optical density was measured at 570 nm. Three independent experiments were conducted.

Western blot analysis

The antibodies used for the Western blot analysis were anti-KDR (IBL), anti–phospho (p)-VEGFR2 (Tyr1175), anti-VEGFR1, anti-p44/42 MAPK (mitogen-activated protein kinase), anti–p-p44/42 MAPK, anti–c-Kit, anti-PDGFRβ, anti-FGFR1, 2, and 3, horseradish peroxidase–conjugated secondary antibody (Cell Signaling Technology), and anti–β-actin (Santa Cruz Biotechnology). The methods have been previously described (18). Two independent immunoblotting experiments were conducted.

Tube formation assay

HUVECs were cultured without VEGF-A for 24 hours. A total of 40 μL of Matrigel (BD Bioscience) and 20 μL of PBS were mixed and incubated in 96-well plates. After the gel had solidified, a 100-μL volume of HUVECs (2×10^4 cells/well) was seeded onto the plates with 20 ng/mL of VEGF-A and the indicated concentration of BIBF 1120. The 96-well plates were then incubated for 4 hours. Capillary morphogenesis was evaluated under a microscope (Olympus). This assay was carried out in 3 independent experiments.

Real-time reverse transcriptase PCR

The method has been previously described (17). The primers used for real-time reverse transcriptase PCR (RT-PCR) are shown in Supplementary Table 1. *GAPD* was used to normalize the expression levels in the subsequent quantitative analyses.

Flow cytometric analysis for HUVECs

HUVECs were seeded on 6-well plates without VEGF-A for 24 hours. After exposure to BIBF 1120, AG1478, or 5FU for 3 hours, the cells were stimulated with 20 ng/mL of VEGF-A for 30 minutes. The flow cytometric procedure was carried out according to the manufacturer's protocols,

Published OnlineFirst December 3, 2010; DOI:10.1158/1078-0432.CCR-09-2755

using the Fixation/Permeabilization Kit (BD Biosciences); the data were obtained using a FACSCalibur flow cytometer (BD Biosciences). Anti-phosphotyrosine (pTyr) antibody (P-Tyr-100; Cell Signaling) was used to detect the phosphorylation levels.

Flow cytometric analysis for PBLs in the *in vivo* model

In the *in vivo* model, about 0.5 to 1 mL of peripheral blood was obtained from treated mice and 20 ng/ mL of VEGF was added to the whole blood samples for 20 minutes. The red cells were then lysed using a lysis buffer (155 mmol/L NH_4Cl, 10 mmol/L $NaHCO_3$, and 1 mmol/L EDTA2Na, pH 7.3) for 10 minutes, and leukocytes were fixed and permeabilized using a Fixation/Permeabilization Kit for analysis. The following antibodies were used: anti-mouse CD45-PerCP, anti-mouse Flk-1-PE (BD Biosciences), anti-pTyr (P-Tyr-100; Cell Signaling), and Alexa Fluor Mouse IgG1 Isotype Control (BD Parmingen). The analysis was carried out using the WinMDI software (20).

HCC xenograft model

Nude mice (BALB/c nu/nu; 6-wk-old females; CLEA Japan Inc.) were used for the *in vivo* studies and were cared for in accordance with the recommendations for the handling of laboratory animals for biomedical research, compiled by the Committee on Safety and Ethical Handling Regulations for Laboratory Animal Experiments, Kinki University. The ethical procedures followed and met the requirements of the United Kingdom Coordinating Committee on Cancer Research Guidelines.

Mice were subcutaneously inoculated with a total of 6×10^6 HepG2 cells. Two weeks after inoculation, the mice were randomized according to tumor size into 3 groups to equalize the mean pretreatment tumor size among the 3 groups ($n = 6$ in each group). The mice were then treated with BIBF 1120 (50 mg/kg/d, p.o.), BIBF 1120 (100 mg/kg/d, p.o.), or the vehicle control (saline, p.o.) for 14 days (Fig. 3A–C). On day 14, the mice were euthanized, blood samples were collected by cardiac puncture, and tumor specimens were collected for immunohistochemistry. The tumor volume was calculated as the length $\times$ width$^2 \times 0.5$ and was assessed every 2 to 3 days.

Immunohistochemical analysis

A mouse anti-CD31 monoclonal antibody (1:100; BD Biosciences) was used to detect the endothelial cells. The paraffin-embedded samples were cut into 4-μm sections, deparaffinized, and placed in a preheated antigen retrieval solution (Dako) in a steamer for 10 minutes. All the samples were then blocked in 3% H_2O_2 in methanol for 15 minutes and rinsed with PBS. The slides were then placed in a Sequenza slide staining system (Thermo Fisher Scientific) and blocked in 1% normal goat serum for 20 minutes. The slides were incubated overnight at 4°C with the CD31 antibody. A standard avidin–biotin peroxidase complex assay was then carried out using the ABC Elite Kit (Vector Laboratories). The slides were developed with 3,3′-diaminobenzidine (DAB; Zymed Laboratories) and counterstained with 10% hematoxylin. Microvessel density (MVD) was quantified by measuring the number of CD31-positive endothelial cells in the tumors. Ten random fields per tumor sample at 200× magnification were captured and saved for computer-assisted image analysis using the ImageJ software package (21). An algorithm for color deconvolution was used to segregate the brown DAB-positive CD31 endothelial cells and the blue tumor cells. Thresholds were adjusted to remove background and nonspecific signals. MVD was reported as the average ratio of CD31-positive cells to tumor cells.

Statistical analysis

The statistical analyses were carried out using Microsoft Excel (Microsoft) to calculate the SD and to test for statistically significant differences between the samples using a Student's t test. A value of $P < 0.05$ was considered statistically significant.

Results

BIBF 1120 potently inhibits VEGFR2 signaling in HUVECs

We evaluated the inhibitory effect of BIBF 1120 at various concentrations (0.0001–10 μmol/L) on VEGFR2 signaling, using HUVECs stimulated with 20 ng/mL of VEGF. BIBF 1120 at a concentration of 0.01 μmol/L completely inhibited the phosphorylation of VEGFR2 and MAPK in HUVECs (Fig. 1A). BIBF 1120 at a concentration of 0.01 μmol/L partially inhibited tube formation in HUVECs stimulated with VEGF, whereas BIBF 1120 at a concentration of 1 μmol/L completely inhibited tube formation (Fig. 1B). These data indicate that BIBF 1120 potently inhibits VEGFR2 signaling in endothelial cells.

Flow cytometry detects BIBF 1120–induced inhibition of pTyr levels

To detect the BIBF 1120–induced inhibition of pTyr levels by flow cytometry, the VEGF-induced pTyr levels of proteins in HUVECs were evaluated after exposure to BIBF 1120, the EGFR TKI AG1478 as a TKI control, or 5FU as a cytotoxic drug control. The controls agents were used to show that another target of TKI did not induce (AG1478) or to exclude the possibility that nonspecific effects such as cytotoxic cellular responses were not induced (5FU). Flow cytometry revealed that the VEGF-induced pTyr levels in HUVECs were significantly inhibited by BIBF 1120 at concentration of 1 and 5 μmol/L but not by AG1478 or by 5FU (Fig. 1C and D). This flow cytometric method is considered a feasible means of detecting the inhibition of VEGF-induced pTyr levels induced by VEGFR2 TKIs.

Growth inhibitory effects and expression status of targeted receptors in HCC cell lines *in vitro*

To evaluate the expression status of the putative targeted receptors of BIBF 1120 in the 4 HCC cell lines and HUVECs as a control, we examined the protein expression levels of VEGFR1, VEGFR2, FGFR1, FGFR2, FGFR3, PDGFRβ, and

Published OnlineFirst December 3, 2010; DOI:10.1158/1078-0432.CCR-09-2755

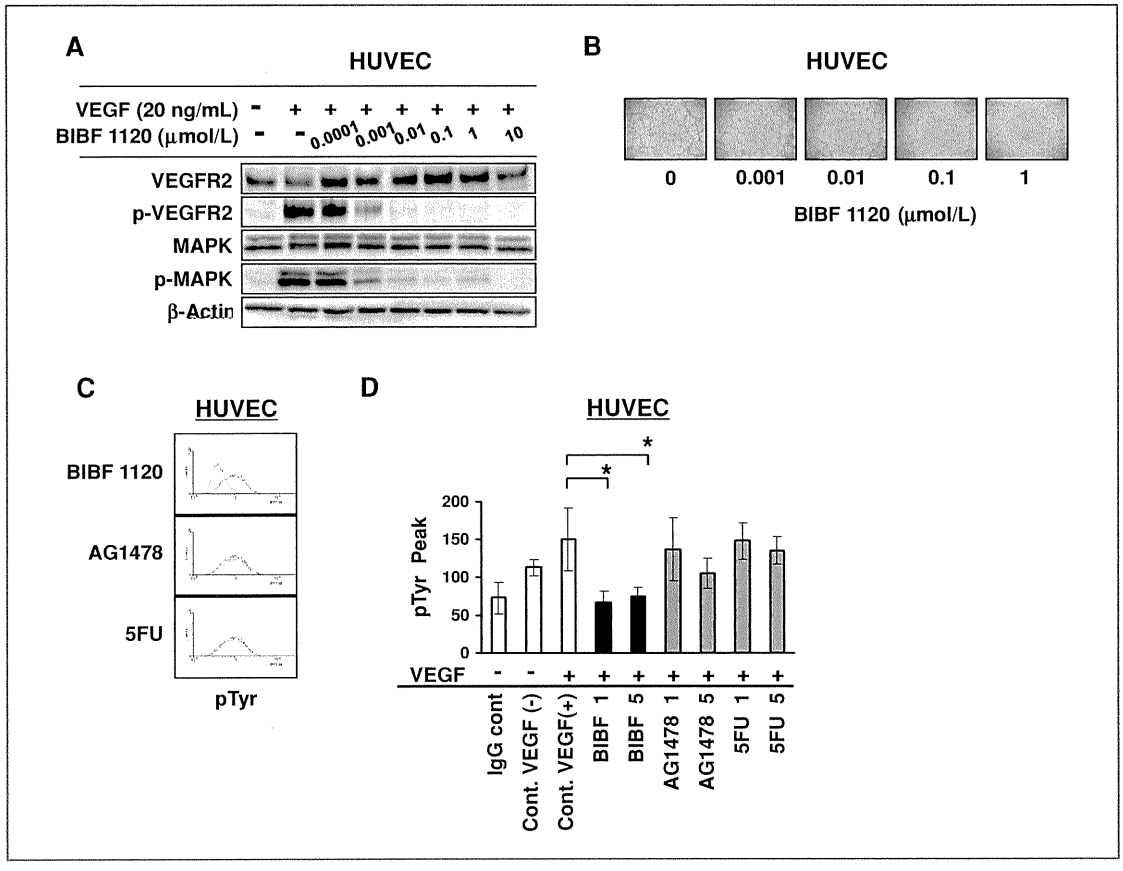

Figure 1. Inhibition of VEGFR2 signaling by BIBF 1120 and detection of the inhibition of pTyr by flow cytometry in HUVECs. A, the inhibition of VEGFR2 and MAPK phosphorylation by BIBF 1120 was determined using a Western blot analysis. HUVECs cultured in a medium containing 2% FBS were exposed to BIBF 1120 (0.0001–10 μmol/L) for 3 hours, stimulated with 20 ng/mL of VEGF for 15 minutes, and lysed for analysis. B, effect of BIBF 1120 on the inhibition of tube formation. HUVECs were seeded with 20 ng/mL of VEGF-A and exposed to BIBF 1120 (0.001–1 μmol/L) on Matrigel-layered 96-well plates for 4 hours. Capillary morphogenesis was evaluated under a microscope. This assay was conducted in 3 independent experiments. C and D, HUVECs were seeded on 6-well plates without VEGF-A for 24 hours. After exposure to BIBF 1120, AG1478, or 5FU for 3 hours, the cells were stimulated with 20 ng/mL of VEGF-A for 30 minutes. The inhibition of pTyr level was detected by flow cytometry with an anti-pTyr antibody. Note that only BIBF 1120 significantly inhibited the VEGF-induced phosphorylation levels of tyrosine. This assay was conducted in 3 independent experiments; bars, SD. *, $P < 0.05$.

c-Kit (the kinase activities of which are reportedly inhibited by BIBF 1120 (15) and p-VEGFR2, MAPK, and p-MAPK by Western blotting. The protein expression of these receptors were not highly upregulated in any of the HCC cell lines, except for PDGFRβ in HLE and HLF cells (Fig. 2A). A comparable expression level of MAPK was observed among the cell lines, and an increase in p-MAPK expression was observed in HLE cells. The mRNA expression levels of the target receptors *VEGFR1*, *VEGFR2*, *VEGFR3*, *PDGFRA*, *PDGFRB*, *FGFR1*, *FGFR2*, *FGFR3*, and *FGFR4* were determined using real-time RT-PCR in the HUVEC line and the HCC cell line. Higher receptor expression levels were observed for *VEGFR2* in HUVECs, *PDGFRB* in HLE and HLF, *FGFR1* in HUVECs and HLE, *FGFR3* in HepG2, and *FGFR4* in Huh7 (Fig. 2B). The expression levels were consistent with the Western blotting results.

We next evaluated the direct growth inhibitory activity of BIBF 1120 in 4 HCC cell lines *in vitro*. The IC_{50} value of BIBF 1120 for the HLE, HLF, HepG2, and Huh7 cell lines were 2.7 ± 1.7, 2.7 ± 0.5, 5.3 ± 0.6, and 4.3 ± 0.9 μmol/L, respectively (Fig. 2C). These results indicate that the direct growth inhibitory activity of BIBF 1120 against HCC cells was relatively mild (IC_{50}: 2–5 μmol/L).

BIBF 1120 potently inhibits tumor growth and angiogenesis of HCC xenografts *in vivo*

Next, we examined the antitumor and antiangiogenic effects of BIBF 1120 *in vivo*. Mice inoculated with HepG2

Published OnlineFirst December 3, 2010; DOI:10.1158/1078-0432.CCR-09-2755

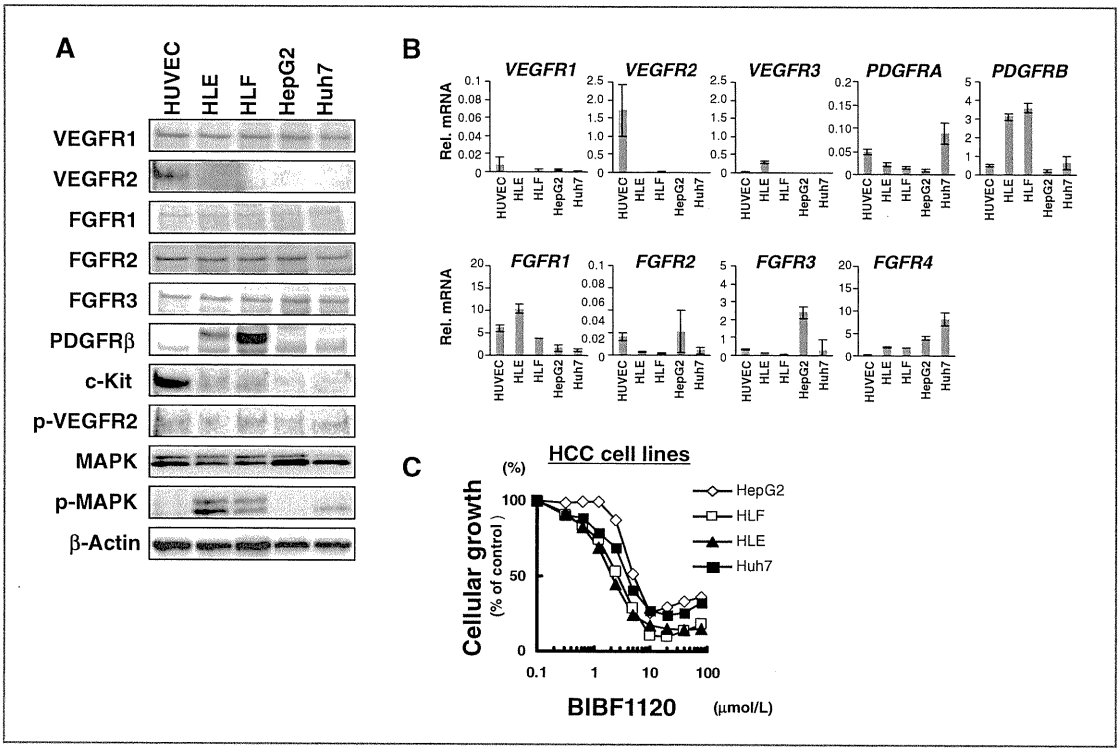

Figure 2. Expression levels of target receptors and sensitivity to BIBF 1120 in HCC cell lines. A, Western blot analysis of the expression levels of VEGFR1, VEGFR2, FGFR1, FGFR2, FGFR3, PDGFRβ, c-Kit, p-VEGFR2, MAPK, p-MAPK, and β-actin in HCC cell lines and HUVECs as a control. B, the mRNA expression levels of *VEGFR1*, *VEGFR2*, *VEGFR3*, *PDGFRA*, *PDGFRB*, *FGFR1*, *FGFR2*, *FGFR3*, and *FGFR4* were determined using real-time RT-PCR. Rel mRNA, mRNA expression levels normalized using *GAPD* (target gene/GAPD $\times 10^3$). C, *in vitro* growth inhibitory effect of BIBF 1120 in 4 HCC cell lines by an MTT assay; bars, SD of 3 independent experiments. This assay was conducted in 3 independent experiments.

cells were orally given a low (50 mg/kg/d) or high (100 mg/kg/d) dose of BIBF 1120, or vehicle alone, for 2 weeks (Fig. 3A). The mean tumor volumes on day 14, for each group of mice, were as follows: vehicle alone, 1,367 ± 634 mm^3; 50 mg/kg/d, 488 ± 489 mm^3; and 100 mg/kg/d, 572 ± 556 mm^3. Both doses of BIBF 1120 significantly inhibited tumor growth ($T/C = 0.36$ and 0.42, respectively), indicating that BIBF 1120 has a potent antitumor activity against HCC *in vivo* (Fig. 3B). Body weight loss was not observed after the administration of BIBF 1120 at either dose (Supplementary Fig. S1). The CD31 staining of tumor tissues showed that BIBF 1120 administration also significantly inhibited tumor angiogenesis (Fig. 3C). Combined with the observation of the direct growth inhibitory activity against HCC *in vitro*, these findings suggest that the antitumor activity of BIBF 1120 *in vivo* mainly result from the drug's antiangiogenic activity, which blocks VEGF signaling.

VEGFR2$^+$pTyr$^+$ PBLs are a pharmacodynamic biomarker *in vivo*

VEGFR2$^+$CD45^{dim} PBLs are generally regarded as circulating endothelial cells (22); therefore, we hypothesized that VEGFR2$^+$CD45^{dim} PBLs might be useful as a biological biomarker of VEGFR2 TKIs. The effects of BIBF 1120 on the pTyr levels of VEGFR2$^+$CD45^{dim} PBLs and the percentage of VEGFR2$^+$pTyr$^+$ PBLs was examined *in vivo* (Fig. 4A). Murine blood samples were obtained from tumor-bearing, BIBF 1120–treated mice, as described previously. The pTyr levels of the VEGFR2$^+$CD45^{dim} PBLs were significantly inhibited by BIBF 1120 treatment, but the difference was relatively small (Fig. 4B and C). On the other hand, the percentage of VEGFR2$^+$pTyr$^+$ PBLs was markedly decreased by BIBF 1120 administration (Cont: 1.8% ± 1.1%, B50: 0.34% ± 0.21%, B100: 0.37% ± 0.29%; Fig. 5A and B). These findings raise the possibility that evaluating the VEGFR2$^+$CD45^{dim} PBLs by flow cytometry as a surrogate tissue may contribute to the proof of concept of VEGFR2-targeting drugs or the monitoring of drug effects *in vivo*. Thus, VEGFR2$^+$pTyr$^+$ PBLs might be a useful pharmacodynamic biomarker of VEGFR2 TKIs in early clinical trials.

Discussion

HCC is one of the most hypervascular tumors, and vascular embolization has been used as a therapeutic strategy. A recent study showed that sorafenib exhibits

Published OnlineFirst December 3, 2010; DOI:10.1158/1078-0432.CCR-09-2755

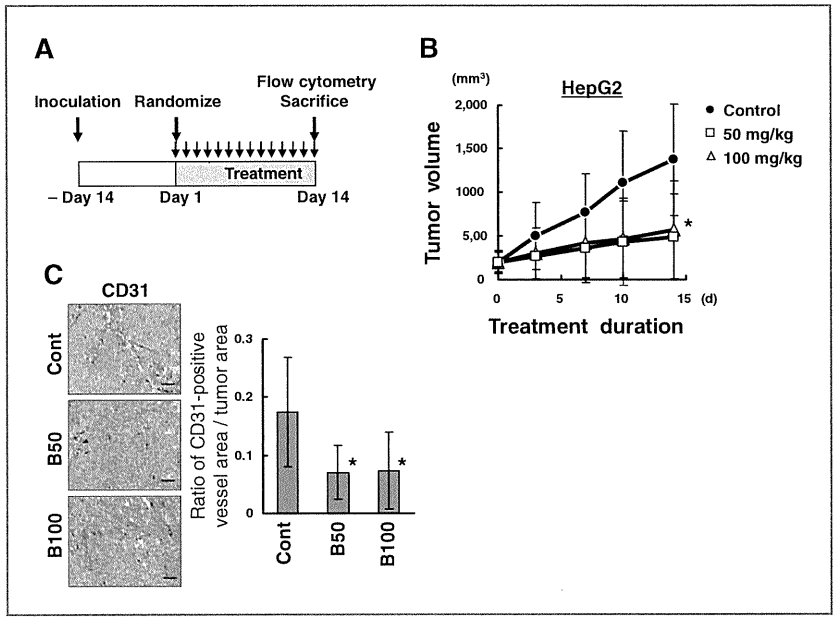

Figure 3. BIBF 1120 exhibited the antitumor and antiangiogenic effects against HCC *in vivo*. A, schema of the BIBF 1120 treatment schedules. Mice were inoculated with HepG2 cells for 14 days. The mice were then randomized into 3 groups ($n = 6$ in each group) and treated with BIBF 1120 (50 mg/kg/d, p.o.), BIBF 1120 (100 mg/kg/d, p.o.), or the vehicle control (p.o.) for 14 days. On day14, the mice were euthanized; blood was collected for the following biomarker study, and tumor specimens were collected for immunohistochemistry. B, inhibition of tumor growth by BIBF 1120 treatment. The tumor volume was assessed every 2 to 3 days ($n = 6$ in each group). Bars, SD. *, $P < 0.05$. C, inhibition of tumor angiogenesis by BIBF 1120 treatment was evaluated using the CD31 staining of tumor samples. Representative data are shown. MVD was quantified by measuring the number of CD31-positive endothelial cells in the tumors. Ten random fields per tumor sample at a magnification of ×200 were captured and saved for computer-assisted image analysis using the ImageJ software package. The *y*-axis represents the ratio of the CD31-positive vessel area/tumor area. Scale bar, 100 μm. Cont, tumor sample treated with vehicle control. B50 and B100, tumor sample treated with BIBF 1120 (50 mg/kg/d, 100 mg/kg/d, p.o.); *, $P < 0.05$.

clinical benefits in patients with advanced HCC (2, 3). This encouraging result suggests that molecular targeting drugs might be active against HCC, especially those that block VEGFR signaling. Our data showed that BIBF 1120 inhibited tumor growth and angiogenesis in HCCs *in vivo*, suggesting that BIBF 1120 may be an active and promising drug against HCC.

BIBF 1120 has a potent inhibitory effect on VEGFRs, similar to that of sorafenib and sunitinib, and it also has activities against FGFRs and Src (refs. 15, 23, 24; Supplementary Table S2). Recent evidence has shown that Src expression is elevated and active in HCC and that Src may play a key role in supporting HCC progression (25); furthermore, HBx increased the activation of the androgen receptor through c-Src kinase, which acts as a major switch in the activation of HCC (26). We conducted a Western blot analysis to detect the inhibitory effect of BIBF 1120 on Src activity, using HUVECs and HepG2, Huh7, HLE, and HLF cells (Supplementary Fig. S2). The inhibitory effect of BIBF 1120 on p-Src was observed in HUVECs and HLE and HepG2 cells, suggesting that BIBF 1120 actually has an inhibitory effect on Src. This effect may benefit HCC therapy in a manner independent of its antiangiogenic effect, although this topic needs to be further investigated. Similarly, we showed an inhibitory effect of BIBF 1120 on p-FGFR2 by using FGFR2-amplified gastric cancer cell lines (Supplementary Fig. S3). Brivanib (BMS-540215), a dual inhibitor of VEGFR and FGFR, is currently in development for the treatment of HCC and colon carcinoma, and preclinical studies have shown that FGFR signaling in HCC cells seems to be a promising therapeutic target (27, 28). These results suggest that the effect of BIBF 1120 on FGFR may contribute the antitumor effect, although further investigation is needed.

Numerous candidate biomarkers of angiogenesis have been identified, but the use of these markers for diagnosis, prognosis, and treatment monitoring remains investigational and of uncertain utility (4). Among them, biomarkers for detecting the blockade of VEGFR signaling have received particular attention because of the intimate involvement of this mechanism in drug activity of VEGFR TKIs. We have shown that VEGF-induced $VEGFR2^{+}pTyr^{+}$ PBLs in peripheral blood samples were markedly decreased by BIBF 1120 treatment *in vivo*. This analysis was done using only peripheral blood collection, VEGF stimulation, and analysis of 2-color flow cytometry; thus, this method is feasible

Published OnlineFirst December 3, 2010; DOI:10.1158/1078-0432.CCR-09-2755

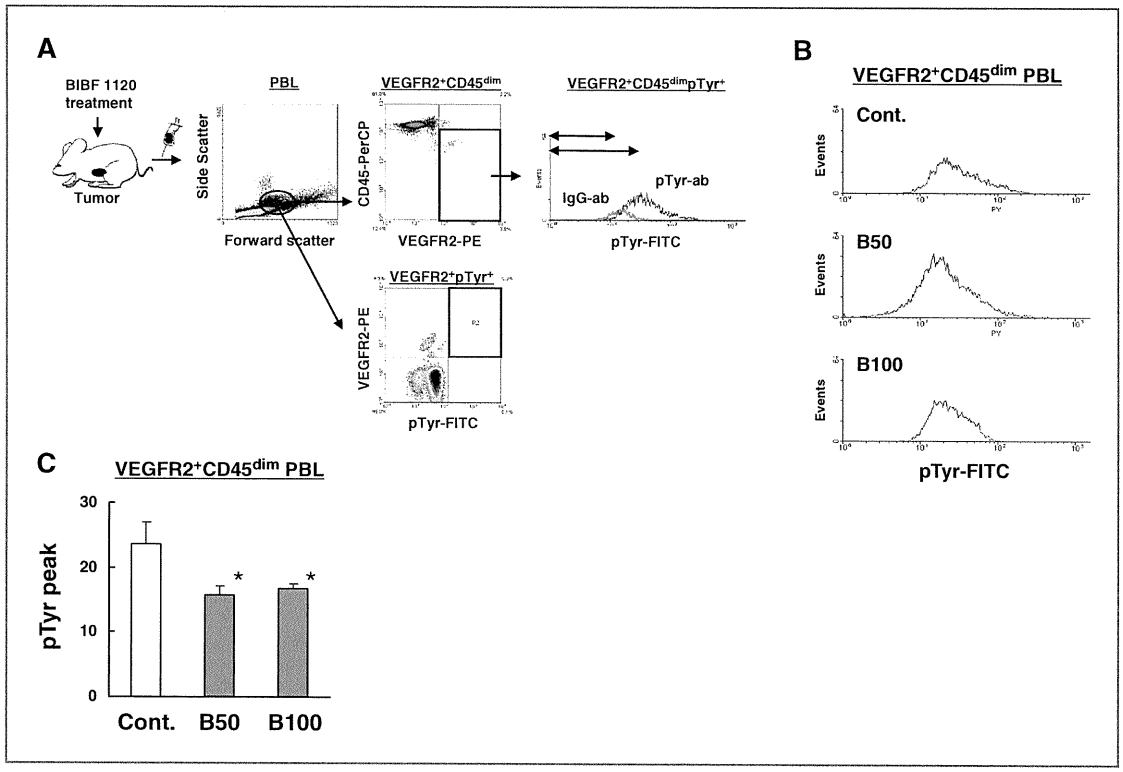

Figure 4. Evaluation of VEGFR2$^+$CD45^{dim} PBLs as a biomarker *in vivo*. A, schema of treatment schedules of BIBF 1120 and detection methods. Peripheral blood samples obtained from BIBF 1120–treated mice were stimulated with 20 ng/mL of VEGF for 30 minutes. The cells were fixed, permeabilized, and reacted with the following antibodies: anti-mouse CD45-PerCP, anti-mouse Flk-1-PE, and anti-pTyr-FITC (fluorescein isothiocyanate). Two methods, the tyrosine phosphorylation levels of VEGFR2$^+$CD45^{dim} PBLs and the percentage of VEGFR2$^+$pTyr$^+$ PBLs, were examined. B and C, BIBF 1120 significantly inhibited the pTyr levels of VEGFR2$^+$CD45^{dim} PBLs *in vivo*. Cont, blood sample from vehicle control. B50 and B100, blood samples from BIBF 1120 (50 mg/kg/d, 100 mg/kg/d; p.o.) treatment groups; bars, SD. *, $P < 0.05$.

and specific to VEGF signaling. Our method may contribute to the proof of concept for VEGFR2 TKIs and may help to determine the biological optimal dose, especially in phase I clinical trials.

Phase II studies of BIBF 1120 against lung cancer and ovarian cancer have been completed and phase I/II study of BIBF 1120 is currently evaluated in HCC (NCT 01004003). Two large phase III clinical trials against lung cancer

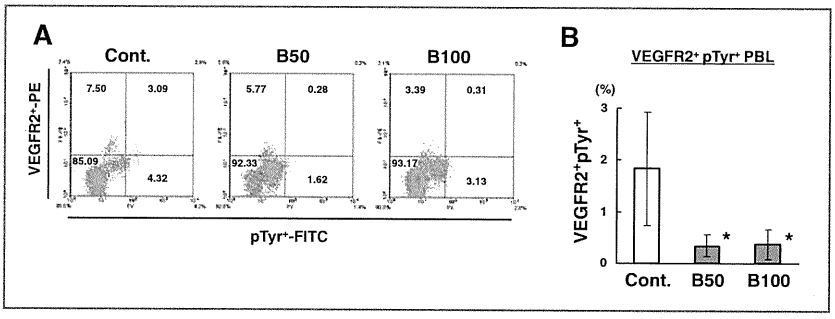

Figure 5. VEGFR2$^+$pTyr$^+$ PBLs can be used as a pharmacodynamic biomarker *in vivo*. A, the percentage of VEGFR2$^+$pTyr$^+$ PBLs obtained from BIBF 1120–treated mice. The numeral data indicate the percentage (%) in each quadrant. Representative data are shown. B, BIBF 1120 significantly inhibited the percentage of VEGFR2$^+$pTyr$^+$ PBLs. Cont, blood samples from vehicle control group ($n = 6$, not treated with drug). B50 and B100, blood samples from BIBF 1120 treatment groups ($n = 6$, 50 mg/kg/d; $n = 6$, 100 mg/kg/d; p.o.); bars, SD. *, $P < 0.05$.

Published OnlineFirst December 3, 2010; DOI:10.1158/1078-0432.CCR-09-2755

(LUME-Lung 1: docetaxel ± BIBF 1120; LUME-Lung 2: pemetrexed ± BIBF 1120) and 1 against ovarian cancer (LUME-Ovar 1: carboplatin/paclitaxel ± BIBF 1120) are now underway. We have shown that BIBF 1120 exhibited antiangiogenic and antitumor activity against HCC *in vivo*. These results may provide the scientific rationale for introducing BIBF 1120 as a treatment of HCC in the future. In addition, our approach of evaluating $VEGFR2^{+}pTyr^{+}$ PBLs in VEGFR TKI might be applicable to future phase I trials. We plan to use this method in clinical settings.

In conclusion, BIBF 1120 clearly inhibited VEGFR2 signaling in endothelial cells and exhibited relatively mild growth inhibitory effects on 4 HCC cell lines (IC_{50} values: 2–5 μmol/L) *in vitro*. BIBF 1120 exhibited potent antitumor and antiangiogenic activities against HCC *in vivo*, and the antitumor effect did not fail or show signs of weakening during the long-term administration period. In addition, $VEGFR2^{+}pTyr^{+}$ PBLs were found to be a noninvasive pharmacodynamic biomarker in a murine model.

Disclosure of Potential Conflicts of Interest

No potential conflicts of interest were disclosed.

Acknowledgment

We thank Mr. Shinji Kurashimo (Life Science Research Institute, Kinki University) for technical assistance.

Grant Support

This work was supported by funds for the Comprehensive Third Term of the 10-Year Strategy for Cancer Control, the program for the promotion of Fundamental Studies in Health Sciences of the National Institute of Biomedical Innovation (NiBio), a grant-in-aid for Scientific Research from the Ministry of Education, Culture, Sports, Science and Technology of Japan (19209018), and a fund from the Health and Labor Scientific Research Grants (20-9).

The costs of publication of this article were defrayed in part by the payment of page charges. This article must therefore be hereby marked *advertisement* in accordance with 18 U.S.C. Section 1734 solely to indicate this fact.

Received October 15, 2009; revised October 1, 2010; accepted November 24, 2010; published OnlineFirst December 23, 2010.

References

1. Ma WW, Adjei AA. Novel agents on the horizon for cancer therapy. CA Cancer J Clin 2009;59:111–37.
2. Llovet JM, Ricci S, Mazzaferro V, Hilgard P, Gane E, Blanc JF, et al. Sorafenib in advanced hepatocellular carcinoma. N Engl J Med 2008;359:378–90.
3. Cheng AL, Kang YK, Chen Z, Tsao CJ, Qin S, Kim JS, et al. Efficacy and safety of sorafenib in patients in the Asia-Pacific region with advanced hepatocellular carcinoma: a phase III randomised, double-blind, placebo-controlled trial. Lancet Oncol 2009;10:25–34.
4. Brown AP, Citrin DE, Camphausen KA. Clinical biomarkers of angiogenesis inhibition. Cancer Metastasis Rev 2008;27:415–34.
5. Kummar S, Kinders R, Rubinstein L, Parchment RE, Murgo AJ, Collins J, et al. Compressing drug development timelines in oncology using phase "0" trials. Nat Rev Cancer 2007;7:131–9.
6. Sessa C, Guibal A, Del Conte G, Rüegg C. Biomarkers of angiogenesis for the development of antiangiogenic therapies in oncology: tools or decorations? Nat Clin Pract Oncol 2008;5:378–91.
7. Jubb AM, Hurwitz HI, Bai W, Holmgren EB, Tobin P, Guerrero AS, et al. Impact of vascular endothelial growth factor-A expression, thrombospondin-2 expression, and microvessel density on the treatment effect of bevacizumab in metastatic colorectal cancer. J Clin Oncol 2006;24:217–27.
8. Poon RT, Fan ST, Wong J. Clinical implications of circulating angiogenic factors in cancer patients. J Clin Oncol 2001;19:1207–25.
9. George DJ, Halabi S, Shepard TF, Vogelzang NJ, Hayes DF, Small EJ, et al. Prognostic significance of plasma vascular endothelial growth factor levels in patients with hormone-refractory prostate cancer treated on cancer and leukemia group B 9480. Clin Cancer Res 2001;7:1932–6.
10. Nishimura R, Nagao K, Miyayama H, Matsuda M, Baba K, Yamashita H, et al. Higher plasma vascular endothelial growth factor levels correlate with menopause, overexpression of p53, and recurrence of breast cancer. Breast Cancer 2003;10:120–8.
11. Werther K, Christensen IJ, Nielsen HJ; Danish prognostic impact of matched preoperative plasma and serum VEGF in patients with primary colorectal carcinoma. Br J Cancer 2002;86:417–23.
12. Drevs J, Siegert P, Medinger M, Mross K, Strecker R, Zirrgiebel U, et al. Phase I clinical study of AZD2171, an oral vascular endothelial growth factor signaling inhibitor, in patients with advanced solid tumors. J Clin Oncol 2007;25:3045–54.
13. Rini BI, Michaelson MD, Rosenberg JE, Bukowski RM, Sosman JA, Stadler WM, et al. Antitumor activity and biomarker analysis of sunitinib in patients with bevacizumab-refractory metastatic renal cell carcinoma. J Clin Oncol 2008;26:3743–8.
14. Okamoto I, Kaneda H, Satoh T, Okamoto W, Miyazaki M, Morinaga R,, et al. Phase I safety, pharmacokinetic, and biomarker study of BIBF 1120, an oral triple tyrosine kinase inhibitor in patients with advanced solid tumors. Mol Cancer Ther 2010;9:2825–33.
15. Hilberg F, Roth GJ, Krssak M, Kautschitsch S, Sommergruber W, Tontsch-Grunt U, et al. BIBF 1120: triple angiokinase inhibitor with sustained receptor blockade and good antitumor efficacy. Cancer Res 2008;68:4774–82.
16. Kulimova E, Oelmann E, Bisping G, Kienast J, Mesters RM, Schwäble J, et al. Growth inhibition and induction of apoptosis in acute myeloid leukemia cells by new indolinone derivatives targeting fibroblast growth factor, platelet-derived growth factor, and vascular endothelial growth factor receptors. Mol Cancer Ther 2006;5:3105–12.
17. Takeda M, Arao T, Yokote H, Komatsu T, Yanagihara K, Sasaki H, et al. AZD2171 shows potent antitumor activity against gastric cancer over-expressing fibroblast growth factor receptor 2/keratinocyte growth factor receptor. Clin Cancer Res 2007;13:3051–7.
18. Arao T, Fukumoto H, Takeda M, Tamura T, Saijo N, Nishio K. Small in-frame deletion in the epidermal growth factor receptor as a target for ZD6474. Cancer Res 2004;64:9101–4.
19. Arao T, Yanagihara K, Takigahira M, Takeda M, Koizumi F, Shiratori Y, et al. ZD6474 inhibits tumor growth and intraperitoneal dissemination in a highly metastatic orthotopic gastric cancer model. Int J Cancer 2006;118:483–9.
20. Márquez MG, Galeano A, Olmos S, Roux ME. Flow cytometric analysis of intestinal intraepithelial lymphocytes in a model of immunodeficiency in Wistar rats. Cytometry 2000;41:115–22.
21. Ganzer R, Blana A, Gaumann A, Stolzenburg JU, Rabenalt R, Bach T, et al. Topographical anatomy of periprostatic and capsular nerves: quantification and computerized planimetry. Eur Urol 2008;54:353–60.
22. Bertolini F, Shaked Y, Mancuso P, Kerbel RS. The multifaceted circulating endothelial cell in cancer: towards marker and target identification. Nat Rev Cancer 2006;6:835–45.
23. Wilhelm SM, Carter C, Tang L, Wilkie D, McNabola A, Rong H, et al. BAY 43-9006 exhibits broad spectrum oral antitumor activity and targets the RAF/MEK/ERK pathway and receptor tyrosine kinases involved in tumor progression and angiogenesis. Cancer Res 2004;64:7099–109.
24. Mendel DB, Laird AD, Xin X, Louie SG, Christensen JG, Li G, et al. *In vivo* antitumor activity of SU11248, a novel tyrosine kinase inhibitor

Published OnlineFirst December 3, 2010; DOI:10.1158/1078-0432.CCR-09-2755

targeting vascular endothelial growth factor and platelet-derived growth factor receptors: determination of a pharmacokinetic/pharmacodynamic relationship. Clin Cancer Res 2003;9:327–37.

25. Lau GM, Lau GM, Yu GL, Gelman IH, Gutowski A, Hangauer D, et al. Expression of Src and FAK in hepatocellular carcinoma and the effect of Src inhibitors on hepatocellular carcinoma *in vitro*. Dig Dis Sci 2009;54:1465–74.
26. Yang WJ, Chang CJ, Yeh SH, Lin WH, Wang SH, Tsai TF, et al. Hepatitis B virus X protein enhances the transcriptional activity of the androgen receptor through c-Src and glycogen synthase kinase-3beta kinase pathways. Hepatology 2009;49:1515–24.
27. Marathe PH, Kamath AV, Zhang Y, D'Arienzo C, Bhide R, Fargnoli J. Preclinical pharmacokinetics and *in vitro* metabolism of brivanib (BMS-540215), a potent VEGFR2 inhibitor and its alanine ester prodrug brivanib alaninate. Cancer Chemother Pharmacol 2009;65:55–66.
28. Huynh H, Ngo VC, Fargnoli J, Ayers M, Soo KC, Koong HN, et al. Brivanib alaninate, a dual inhibitor of vascular endothelial growth factor receptor and fibroblast growth factor receptor tyrosine kinases, induces growth inhibition in mouse models of human hepatocellular carcinoma. Clin Cancer Res 2008;14:6146–53.

J Gastroenterol (2011) 46:212–221
DOI 10.1007/s00535-010-0294-5

ORIGINAL ARTICLE—LIVER, PANCREAS, AND BILIARY TRACT

The cancer stem cell marker CD133 is a predictor of the effectiveness of S1+ pegylated interferon α-2b therapy against advanced hepatocellular carcinoma

Satoru Hagiwara · Masatoshi Kudo · Kazuomi Ueshima · Hobyung Chung · Mami Yamaguchi · Masahiro Takita · Seiji Haji · Masatomo Kimura · Tokuzo Arao · Kazuto Nishio · Ah-Mee Park · Hiroshi Munakata

Received: 23 December 2009 / Accepted: 8 July 2010 / Published online: 4 August 2010

Abstract
Background Combination therapy with the oral fluoropyrimidine anticancer drug S1 and interferon is reportedly effective for the treatment of advanced hepatocellular carcinoma (HCC), but selection criteria for this therapy have not been clarified. In this study, we attempted to identify factors predicting the effectiveness of this combination therapy.
Methods Pathological specimens of HCC were collected before treatment from 31 patients with advanced HCC who underwent S1+ pegylated-interferon (PEG-IFN) α-2b therapy between January 2007 and January 2009. In these pathological specimens, the expression levels of CD133, thymidylate synthase (TS), dihydropyrimidine dehydrogenase (DPD), and interferon-receptor 2 (IFNR2) proteins were determined by Western blot assay. The presence or absence of p53 gene mutations was determined by direct sequencing. The relationships between these protein expression levels and the response rate (RR), progression-free survival (PFS), and overall survival (OS) were evaluated.
Results The CD133 protein expression level was significantly lower in the responder group than in the nonresponder group. Comparing the PFS and OS between high- and low-level CD133 expression groups ($n = 13$ and 18, respectively) revealed that both parameters were significantly prolonged in the latter group. The expression levels of TS, DPD, and IFNR2 protein and the presence of p53 gene mutations did not correlate with the RR.
Conclusions CD133 was identified as a predictor of the therapeutic effect of S1+ PEG-IFN α-2b therapy against advanced HCC.

Keywords 5-Fluorouracil · Pegylated interferon · CD133 · Cancer stem cell · Hepatocellular carcinoma

S. Hagiwara · M. Kudo (✉) · K. Ueshima · H. Chung · M. Yamaguchi · M. Takita
Division of Gastroenterology and Hepatology, Department of Internal Medicine, Kinki University School of Medicine, 377-2 Ohno-Higashi, Ōsakasayama, Osaka 589-8511, Japan
e-mail: m-kudo@med.kindai.ac.jp

S. Haji
Department of Surgery, Kinki University School of Medicine, Ōsakasayama, Japan

M. Kimura
Department of Pathology, Kinki University School of Medicine, Ōsakasayama, Japan

T. Arao · K. Nishio
Department of Genome Biology, Kinki University School of Medicine, Ōsakasayama, Japan

A.-M. Park · H. Munakata
Department of Biochemistry, Kinki University School of Medicine, Ōsakasayama, Japan

Abbreviations

5FU	5-Fluorouracil
DPD	Dihydropyrimidine dehydrogenase
HCC	Hepatocellular carcinoma
IFNR2	Interferon-receptor 2
NR	Nonresponder
OS	Overall survival
PD	Progressive disease
PEG-IFN	Pegylated interferon
PFS	Progression-free survival
PR	Partial response
RR	Response rate

SD Stable disease
TS Thymidylate synthase

Introduction

Hepatocellular carcinoma (HCC) is one of the most common malignancies in Asia, including Japan [1, 2], and its prevalence has recently been increasing globally [3]. In most patients, the background of HCC is chronic hepatitis or liver cirrhosis due to hepatitis B or hepatitis C infection. Recently, HCC has increasingly been detected at relatively early stages due to the periodic follow-up of chronic liver disease patients and the development of diagnostic imaging modalities. There have been significant improvements in the treatment of patients with early HCC, and the therapeutic results have been markedly improved by site-specific treatments such as transcatheter arterial chemoembolization, percutaneous ethanol injection therapy, microwave coagulation therapy, and radiofrequency ablation, as well as hepatectomy [4–6].

However, when existing HCC is cured radically, new cancers develop due to the underlying chronic liver disorders. Treatments must then be performed alone or in combination each time a new cancer appears. Repeated treatment often leads to portal vein tumor thrombosis or distant metastasis, making standard treatments difficult to perform. Recently, the treatment efficacy and safety of the molecular targeted drug sorafenib (Nexavar; Bayer HealthCare Pharmaceuticals–Onyx Pharmaceuticals, Leverkusen, Germany) have been reported and the results placed it as a first-line drug [7]. Sorafenib is a small molecule that inhibits tumor-cell proliferation and tumor angiogenesis and increases the rate of apoptosis in a wide range of tumor models. It acts by inhibiting the serine–threonine kinases Raf-1 and B-Raf and the receptor tyrosine kinase activity of vascular endothelial growth factor receptors (VEGFRs) 1, 2, and 3 and platelet-derived growth factor receptor β (PDGFR-β). Llovet et al. [7] reported that sorafenib prolonged median survival and the time to progression by nearly 3 months in about 300 patients with advanced HCC. Although different types of molecular targeted drugs have been under development, there is no treatment option at present for the patients who fail to respond to sorafenib. Thus, second-line treatment for advanced HCC needs to be established.

The oral fluoropyrimidine anticancer drug, S1, includes the dihydropyrimidine dehydrogenase (DPD) inhibitor 5-chloro-2,4-dihydroxypyridine as a component, and this component is expected to exhibit a marked anticancer effect by preventing 5-fluorouracil (5FU) degradation [8–10]. Combination therapy with S-1 and interferon (IFN) has recently been attempted in patients with advanced HCC, and relatively satisfactory results have been reported [11–14]. However, the response rate for this therapy is limited, and the outcome deteriorates in patients resistant to it. Therefore, if the effectiveness of this therapy can be predicted in advance, unnecessary adverse effects can be avoided, and other treatments may be attempted.

We have noted some candidate proteins which may have a possible relationship with the effect of this therapy. The cancer stem-cell marker CD133 [15–18] can reportedly resist anticancer drugs through an intrinsic drug resistance mechanism [19, 20]. Thymidylate synthase (TS) and DPD are enzymes involved in 5FU metabolism, and many reports have suggested their relationship with the therapeutic effects of 5FU in lung [21] and colon cancers [22]. Furthermore, interferon-receptor 2 (IFNR2) is reported to be the most important of the receptors through which IFN acts directly on HCC [23, 24]. Apoptosis is the primary mechanism of the anticancer effect of anticancer drugs, and p53 is closely involved in apoptosis [25–27].

In the present study, we sought to identify factors predicting the effectiveness of S1+ pegylated-interferon (PEG-IFN) α-2b therapy. HCC tissue samples were collected before the therapy was started, the expression levels of CD133, TS, DPD, and IFNR2 proteins were determined by Western blot analysis, and the presence or absence of p53 gene mutations was examined by direct sequencing. We found that the expression level of CD133 was significantly correlated with the therapeutic effect. Thus, measurement of the CD133 expression level before treatment may facilitate prediction of the therapeutic effect and the avoidance of unnecessary adverse effects.

Subjects, materials, and methods

Patients

Between January 2007 and January 2009, a total of 31 patients with refractory HCC that could not be controlled by standard therapeutic modalities (transcatheter arterial chemoembolization, percutaneous ethanol injection therapy, microwave coagulation therapy, radiofrequency ablation, and hepatectomy) underwent S-1 and PEG-IFN α-2b combination therapy. Patient characteristics are shown in Table 1, with more details shown in Table 2. All pathological specimens of HCC were collected by needle biopsy.

Eligibility criteria

Eligibility criteria for the combination therapy included: (1) advanced HCC that was uncontrollable with standard treatment, or HCC with distant metastasis; (2) age <80 years; (3) an Eastern Cooperative Oncology Group performance status of 0 or 1; (4) Child–Pugh grade A; (5) encephalopathy

Table 1 Characteristics of patients treated with combination therapy of S1 and PEG-IFN α-2b

Characteristics	Number of patients
Total	31
Gender	
Male	28
Female	3
Age (years)	
Median	66
Range	30–80
Cause of disease	
HBV	10
HCV	15
Non-HBV, non-HCV	6
Child–Pugh stage	
A	31
BCLC stage	
C (advanced)	31
ECOG performance status	
0	28
1	3

PEG-IFN pegylated interferon, *HBV* hepatitis B virus, *HCV* hepatitis C virus, *BCLC* Barcelona Clinic Liver Cancer Group, *ECOG* Eastern Cooperative Oncology Group

degree 0; (6) leukocyte count >3,000 cells/mm [3]; hemoglobin level >10 g/dl and platelet count >80,000 cells/mm^3; and (7) serum creatinine <1.5 mg/dl, serum aspartate aminotransferase <200 IU/l, serum alanine aminotransferase <200 IU/l, and serum total bilirubin level <3.0 mg/dl. The diagnosis of HCC was made based on the hematoxylin–eosin staining of histopathological specimens in all patients.

Treatment regimen

After the obtaining of informed consent, 31 patients were treated with S-1 (TS1; Taiho Pharmaceutical, Tokyo, Japan) and PEG-IFN α-2b (Pegintron; Schering-Plough, Kenilworth, NJ, USA) combination therapy. S-1 was given orally at a daily dose of 80–120 mg (depending on the body surface area: <1.25 m^2: 80 mg, >1.25 to <1.5 m^2: 100 mg, <1.5 m^2: 120 mg), divided into two equal doses, from days 1 to 28. PEG-IFN α-2b was given subcutaneously at a dose of 50 μg on days 1, 8, 15, and 22. One course consisted of consecutive administration for 28 days followed by a 2-week drug-free interval. The Medical Ethics Committee of Kinki University of Medicine approved the study.

Assessment of response

Responses of HCC patients to the combination therapy were assessed by contrast-enhanced computed tomography after each course. The response was defined according to the Response Evaluation Criteria in Solid Tumours (RECIST). A partial response (PR) was defined as a minimum 30% decrease in the sum of the longest diameters of the target lesions, with the baseline sum of the longest diameters of these lesions as the reference. Progressive disease (PD) was defined as a minimum 20% increase in the sum of the longest diameters of the target lesions. Stable disease (SD) was defined as meeting neither PR nor PD criteria. When the response achieved regarding intrahepatic HCC was different from that for extrahepatic HCC, the poorer one was determined as the achieved response.

Assessment of toxicity

Blood cell counts and biochemical profiles were performed at least once every week. Adverse reactions were assessed using the National Cancer Institute-Common Toxicity Criteria (NCI-CTC, version 3).

Western blot analysis

To prepare tissue lysate, HCC tissue was homogenized with CelLytic-MT Mammalian Tissue Lysis/Extraction reagent (Sigma-Aldrich, St. Louis, MO, USA) along with 2% sodium dodecyl sulfate (SDS) and the protease inhibitor, Complete^{TM} (Roche Diagnostics, Mannheim, Germany), and centrifuged. Equal protein amounts (8 μg) of tissue lysates were electrophoresed through a reducing SDS polyacrylamide gel and electroblotted onto a polyvinylidene difluoride (PVDF) membrane. The membrane was blocked and incubated with polyclonal IgG for TS (1/500; Taiho Pharmaceutical, Tokyo, Japan), DPD (1/3,000; Taiho Pharmaceutical), IFN-α/βR (1/500; Otsuka Pharmaceutical., Tokyo, Japan), CD133 (1/1,000; Cell Signaling Technology, Danvers, MA, USA), and β-actin (1/2,000; Sigma-Aldrich) in Can Get Signal® immunostain solution (TOYOBO, Osaka, Japan). For CD133 detection, lysis of the human colon cancer cells WiDr and DLD1 (positive and negative controls, respectively) was examined. Protein levels were detected using horseradish peroxidase (HRP)-linked secondary antibodies and the ECL-plus System (GE Healthcare, Buckinghamshire, UK).

To evaluate the signal intensity, the obtained Western blot image data were quantified using Image J software (NIH, Bethesda, MD, USA).

Immunohistochemistry

We performed immunohistochemical analysis of paraffin-embedded sections of HCC. Immunohistochemical staining was carried out with antibodies raised against CD133 (1:100), and visualized using the Dako LSAB System-HRP

Table 2 Detailed characteristics and outcomes of patients treated with combination therapy of S1 and PEG-IFN α-2b

Patient no.	Age (years)	Gender	PS	HBs-Ag	HCV-Ab	Type of intrahepatic tumor	Vascular invasion	Metastasis	Tumor grade	Prior treatment	AFP (ng/ml)		DCP (mAU/ml)		Response	Outcome
											Before	After	Before	After		
1	80	M	0	−	−	Nodular	Absence	LN	Poor[a]	OP, TACE	3	3	16	17	PR	21.2 M dead
2	70	M	0	−	−	Nodular	Presence	−	Poor	OP	6	35	5,535	60,413	PD	1.7 M dead
3	66	M	0	−	−	Nodular	Absence	Lung	Moderate[b]	OP, RFA	243	65	74	21	PR	25.4 M alive
4	61	M	0	+	−	Nodular	Absence	LN	Moderate	TACE	474	22	31	13	PR	8.1 M dead
5	62	M	0	+	−	Nodular	Absence	Lung, adrenal	Moderate	OP, HAIC	3,268	1,122	18	21	PD	1.9 M dead
6	67	M	0	+	−	Nodular	Absence	Lung	Moderate	OP, TACE	7,964	8,643	3,124	6,676	PD	1.3 M dead
7	60	M	0	−	+	Nodular	Presence	−	Poor	OP	11	13	19	37	SD	16.7 M alive
8	74	M	1	−	+	Nodular	Absence	−	Poor	OP, TACE	2,242	490	1,147	2,356	PD	3.0 M alive
9	59	F	0	+	−	Nodular	Presence	Lung	Moderate	HAIC	867	536	1,300	413	PR	7.2 M alive
10	70	M	0	−	−	Nodular	Presence	−	Moderate	−	345	26	61,319	1,024	PR	9.2 M alive
11	74	M	0	−	+	Diffuse	Presence	Adrenal	Moderate	HAIC	2,246	1,352	13,303	11,167	PR	6.6 M dead
12	60	M	0	−	+	Diffuse	Presence	−	Moderate	−	51	48	13,007	8,523	PD	3.6 M dead
13	61	M	0	+	−	Nodular	Presence	−	Moderate	−	8	9	476	209	SD	3.8 M alive
14	75	M	0	−	+	Nodular	Absence	LN	Poor	TACE	2,476	11,722	3,711	5,452	NE	0.6 M dead
15	61	M	0	+	−	Nodular	Absence	−	Poor	TACE	251	175	1,470	2,795	PD	3.8 M alive
16	30	M	0	+	−	Nodular	Presence	−	Moderate	−	114,852	79,361	195	183	PR	5.2 M alive
17	80	M	1	−	+	Diffuse	Absence	Lung, LN, bone	Moderate	−	70	106	116,140	306,800	PD	3.2 M dead
18	78	M	1	−	+	Nodular	Presence	Lung	Moderate	−	13,544	10,192	3,401	4,805	PD	2.8 M dead
19	55	M	0	−	+	Nodular	Presence	Lung, LN	Moderate	−	470	468	62,938	31,608	SD	2.0 M dead
20	35	M	0	−	+	Nodular	Presence	−	Moderate	−	91	285	44,951	58,921	PD	2.3 M dead
21	63	M	0	−	+	Nodular	Absence	−	Moderate	OP	1,140	160	412	96	PR	10.2 M alive
22	66	M	0	−	+	Nodular	Absence	−	Poor	TACE	651	872	3,231	5,890	PD	3.1 M dead
23	67	M	0	−	+	Nodular	Absence	Lung	Poor	OP	73	86	16	24	PD	3.1 M dead
24	57	M	0	−	+	Diffuse	Presence	Lung	Moderate	−	154	43	3,891	123	PR	9.5 M alive
25	65	M	0	−	+	Nodular	Absence	Lung	Moderate	OP, TACE	2,118	4,860	45,359	67,894	PD	1.9 M dead
26	51	M	0	+	−	Nodular	Absence	−	Moderate	−	1,111	3,890	240	651	PD	1.9 M dead
27	72	M	0	+	−	Nodular	Presence	Lung	Moderate	TACE	652	612	1,131	980	PD	5.6 M dead
28	74	M	0	+	−	Nodular	Presence	Lung, LN	Moderate	OP, TACE	658	890	2,418	3,168	PD	2.0 M dead
29	75	F	0	−	+	Nodular	Presence	−	Moderate	HAIC	1,153	2,789	11,456	21,998	PD	5.3 M dead
30	68	F	0	−	−	Nodular	Presence	−	Moderate	−	7	7	231	164	PR	16.2 M alive
31	58	M	0	−	−	Nodular	Presence	Lung, adrenal	Poor	TACE	86	58	14,661	11,990	SD	2.0 M alive

PS performance status, *HBs-Ag* hepatitis B surface antigen, *HCV-Ab* anti-hepatitis C virus antibody, *LN* lymph node, *TACE* transcatheter arterial chemoembolization, *RFA* radiofrequency ablation, *HAIC* hepatic arterial infusion chemotherapy using implanted port system, *AFP* alpha-fetoprotein, *DCP* des-gamma-carboxyprothrombin, *OP* operation, *M* months, *PR* partial response, *PD* progressive disease, *SD* stable disease

[a] Poorly differentiated

[b] Moderately differentiated

(Dako, Carpinteria, CA, USA). Sections were counterstained with hematoxylin.

Determination of p53 sequence

Total RNA extracted from HCC tissue using TRIZOL (Invitrogen, Carlsbad, CA, USA) was reverse-transcribed employing the Takara RNA PCR kit (AMV) Ver.3 (Takara, Tokyo, Japan). p53 was amplified using the forward primer 5′-GAGCCGCAGTCAGATCCTA-3′ and the reverse primer 5′-CAGTCTGAGTCAGGCCCTTC-3′, and nested polymerase chain reaction (PCR) was performed using the primers 5′-CCCCTCTGAGTCAGGAAACA-3′ and 5′-TTATGGCGGGAGGTAGACTG-3′. The PCR product was purified and sequenced using BigDye terminator version 3.1 cycle sequencing on an ABI 3100 DNA sequencer (Applied Biosystems, Foster City, CA, USA).

Statistical analysis

Differences between groups were examined for significance using the Mann–Whitney *U*-test and Fishers exact test where appropriate. Multivariate analysis was performed by using a logistic regression model. Cumulative survival and progression-free survival (PFS) curves were constructed using the Kaplan–Meier method and compared using the log-rank test. All the analyses described above were performed using the SPSS program (version 11.5; SPSS, Chicago, IL, USA).

Results

Response

Complete and partial responses were achieved in 0 (0%) and 10 (32.3%) of the 31 patients, respectively. The overall response rate was 32.3%. Stable disease (SD) was noted in 3 patients (9.7%), and the disease control rate (complete response + partial response + SD) was 41.9%. Progressive disease (PD) was noted in 17 patients (54.8%). One patient was excluded from the assessment of response, because the patient died of HCC rupture 17 days after the start of treatment and the computed tomography could not be performed.

Progression-free survival rate and survival assessment

The median PFS was 1.6 months (95% confidence interval [CI] 1.5–1.7 months). The cumulative PFS rates at 6, 12, and 18 months were 38, 19, and 9%, respectively.

All enrolled patients were also included in a survival assessment. Twelve patients were still alive at the end of the observation period (median 8.2 months, range 2–25.4 months), while 19 patients had died. The causes of death were tumor progression ($n = 18$) and infectious lung disease ($n = 1$). The median survival time was 5.3 months (95% CI 1.7–9.0 months). The cumulative survival rates at 6, 12, 18, and 24 months were 44, 35, 35, and 17%, respectively.

Relationship of CD133, TS, DPD, and IFNR2 protein expression levels in HCC with the anticancer effect of the combined therapy

The expression levels of CD133, TS, DPD, and IFNR2 proteins, which were candidate predictive factors for the therapeutic effect, were studied by Western blotting in all specimens. Figure 1 shows the results in five samples from the PR group and four samples from the PD group. The expression level of CD133 was low in the PR group but high in the PD group. However, no marked differences were noted in the expression levels of TS, DPD, or IFNR2 between the two groups.

Next, the relationships of the CD133, TS, DPD, and IFNR2 protein expression levels with the antitumor effect were evaluated. To compare the protein expression levels among specimens, the relative expression level was calculated by dividing the intensity of each signal on Western blotting by the signal intensity of actin, which is an internal control. The CD133 protein expression level was significantly lower in the responder group (median 0.05) than in the nonresponder group (median 0.58) group ($p = 0.005$) (Fig. 2a). In contrast, the TS, DPD, and IFNR2 protein expression levels showed no significant differences between the responder and nonresponder groups (Fig. 2b–d).

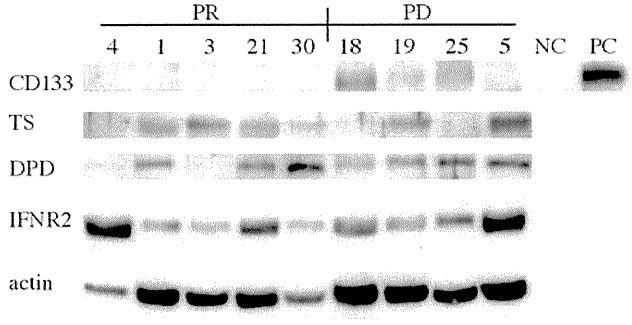

Fig. 1 Expression of CD133, thymidylate synthase (*TS*), dihydropyrimidine dehydrogenase (*DPD*), and interferon receptor 2 (*IFNR2*) as possible factors predicting the therapeutic effect in hepatocellular carcinoma (HCC). Results of Western blotting in typical cases in the partial response (*PR*) and progressive disease (*PD*) groups. For CD133, negative (DLD1) and positive (WiDr) controls were used

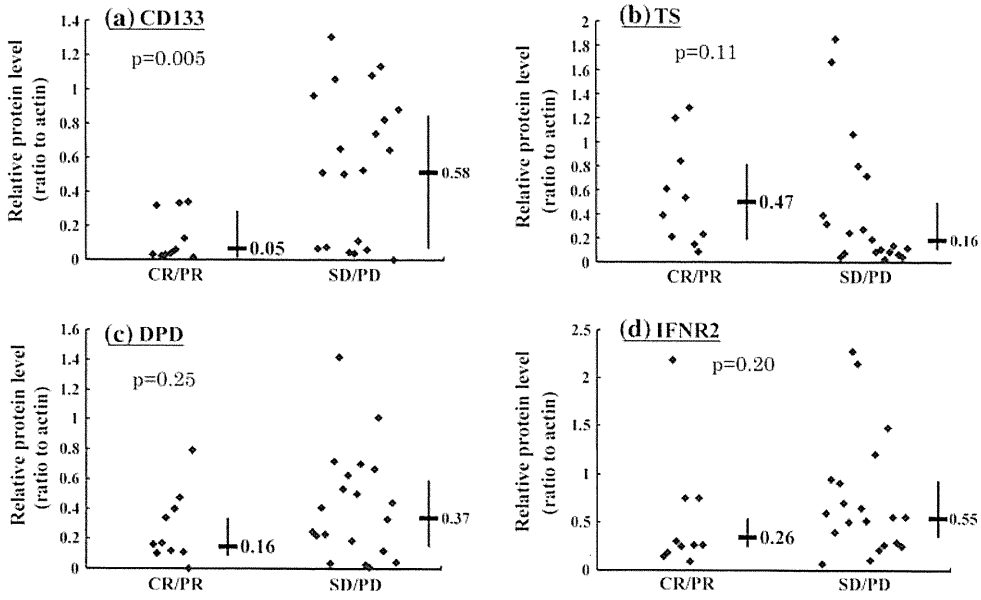

Fig. 2 Relationships between the expression levels of CD133 (**a**), TS (**b**), DPD (**c**), and IFNR2 (**d**) and the anticancer effect. *Vertical lines* on the right of these figures represent the quartile positions, and *horizontal lines* indicate the medians. The numbers of subjects with complete response (*CR*)/PR and stable disease (*SD*)/PD were ten and twenty, respectively

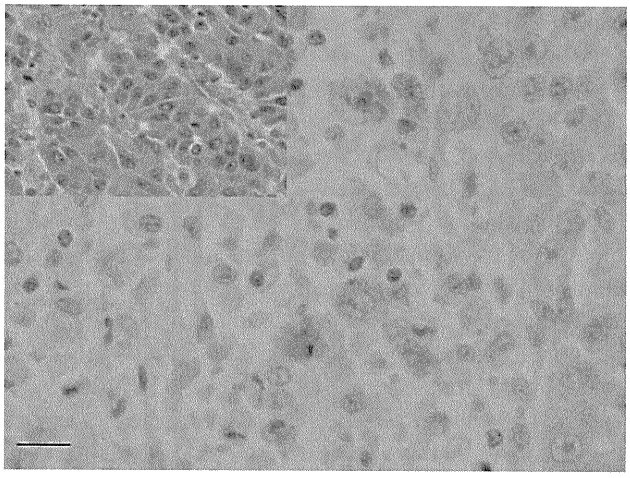

Fig. 3 Immunohistochemistry of CD133 in HCC tissue. This typical sample was intensely positive for CD133. Detection was facilitated using diaminobenzidine (DAB), which shows brown staining when positive. Magnification ×400. *Inset* image is H&E-stained specimen (magnification ×200)

The expression of CD133 was also studied in liver cancer tissues of all specimens using immunohistochemistry. Figure 3 presents specimens that showed intense staining for CD133. The presence or absence of an immunohistological signal was correlated with the CD133 protein expression level determined by Western blotting.

Comparison of the patient background and candidate factors predicting treatment effects with the final outcome (results of univariate analysis and multivariate analysis with a logistic regression model)

Univariate analysis showed a significantly higher CD133 level ($p < 0.01$) in the nonresponder (NR) than the responder group and a slightly higher TS level ($p = 0.11$) in the responder group (Table 3). Using CD133 and TS showing $p < 0.15$ on univariate analysis, multivariate analysis with a logistic regression model was performed. This analysis revealed that only CD133 was a significant factor (odds ratio 0.076, 95% CI 0.007–0.88, $p = 0.039$) (Table 4). Thus, irrespective of the TS level, CD133 was identified as an independent factor predicting the treatment effects.

Relationships of the CD133 protein expression level with the anticancer effect, PFS, and OS

The positive predictive value for nonresponders was 100% in patients whose CD133 expression level exceeded 0.4. Thus, we classified patients into high- and low-CD133 expression groups with a cutoff level of 0.4 (Fig. 2a). Thirteen patients were classified into the high-CD133 expression group and 18 patients into the low-CD133 expression group.

The relationship between the CD133 protein expression level and PFS is shown in Fig. 4. The median PFS was 1.6 months (95% CI 1.5–1.6 months) in the high-CD133 expression group and 7.2 months (95% CI 2–12.3 months) in the low-CD133 expression group. The log-rank test using the Kaplan–Meier method showed that the PFS was significantly prolonged in the low-level compared to the high-level CD133 expression group ($p = 0.036$).

The relationship between the CD133 protein expression level and overall survival (OS) is shown in Fig. 5. The median survival time was 3.1 months (95% CI 1.4–4.8 months) in the high-CD133 expression group, but 8.1 months (95% CI 0–19.3 months) in the low-CD133 expression group. The log-rank test using the Kaplan–Meier

Table 3 Comparison of patient characteristics according to the anticancer effect of the therapy

Variable	Responders (PR) ($n = 10$)	Nonresponders (SD + PD) ($n = 20$)	p value
Age (years)	64.5 (30–80)	65.5 (35–80)	0.85
Sex, no. (%)			0.25
Male	8 (80)	19 (95)	
Female	2 (20)	1 (5)	
Cause of disease, no. (%)			0.21
Hepatitis B	3 (30)	7 (35)	
Hepatitis C	3 (30)	11 (55)	
Non-B, non-C	4 (40)	2 (10)	
ECOG performance status, no. (%)			0.53
0	10 (100)	17 (85)	
1	0 (0)	3 (15)	
Tumor grade, no. (%)			0.21
Moderate	9 (90)	13 (65)	
Poor	1 (10)	7 (35)	
Vascular invasion, no. (%)	6 (60)	11 (55)	1
AFP (ng/ml), median (range)	409.5 (3–114,852)	560.5 (6–13,544)	1
PIVKA II (mAU/ml), median (range)	321.5 (16–61,319)	3,177.5 (16–116,140)	0.17
Previous therapy (last), no. (%)			0.83
OP	2 (20)	4 (20)	
TACE	2 (20)	7 (35)	
HAIC	2 (20)	2 (10)	
None	4 (40)	7 (35)	
CD133, median (range)	0.05 (0.01–0.34)	0.58 (0–1.30)	**<0.01**
IFNR2, median (range)	0.26 (0.09–2.19)	0.55 (0.06–2.27)	0.2
TS, median (range)	0.47 (0.08–1.29)	0.16 (0.03–1.85)	**0.11**
DPD, median (range)	0.16 (0–0.79)	0.37 (0–1.42)	0.25
p53 mutation, no. (%)	1 (10)	2 (10)	1

Values in bold are statistically significant

PR partial response, *SD* stable disease, *PD* progressive disease, *ECOG* Eastern Cooperative Oncology Group, *AFP* alpha-fetoprotein, *TACE* transcatheter arterial chemoembolization, *HAIC* hepatic arterial infusion chemotherapy using implanted port system, *IFNR2* interferon-receptor 2, *TS* thymidylate synthase, *DPD* dihydropyrimidine dehydrogenase, *PIVKA II* protein induced by vitamin K antagonist II

Table 4 Multivariate analysis with a logistic regression model

	Odds ratio	95% CI	p value
CD133 > 0.34	0.076	0.007–0.88	0.039
TS > 0.2	1.643	0.189–14.29	0.653

Cutoff value for each factor was determined by receiver operating characteristic curve (ROC) analysis

CI confidence interval

method showed that, in the low-level CD133 expression group, the OS was significantly prolonged compared to that in the high-level group ($p = 0.022$).

Relationship between p53 mutations and the anticancer effect

Mutant p53 was observed in 3 of the 31 patients. The response rate was 32.1% in the wild-type and 33.3% in the mutant specimens, with no significant difference. The disease control rate was 39.3% in the wild-type and 66.7% in the mutant specimens, with no significant difference.

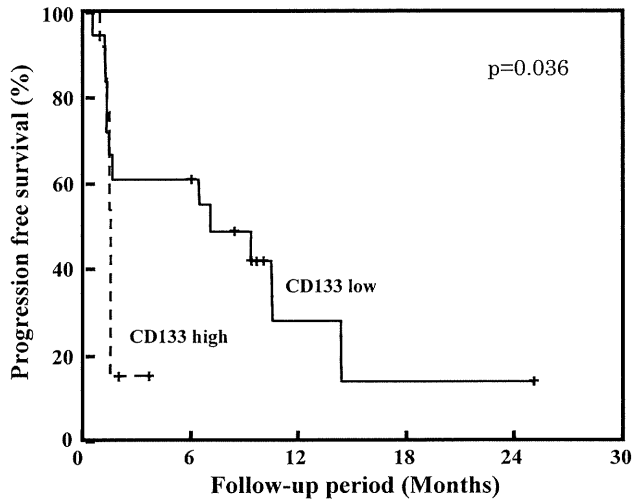

Fig. 4 Progression-free survival of patients who received combination therapy with S-1 and pegylated interferon (PEG-IFN) α-2b, stratified according to the CD133 expression level. Patients were divided into high- and low-CD133 expression groups, with a cutoff value of 0.4 (Fig. 2a). Thirteen and 18 patients belonged to the high- and low-expression groups, respectively

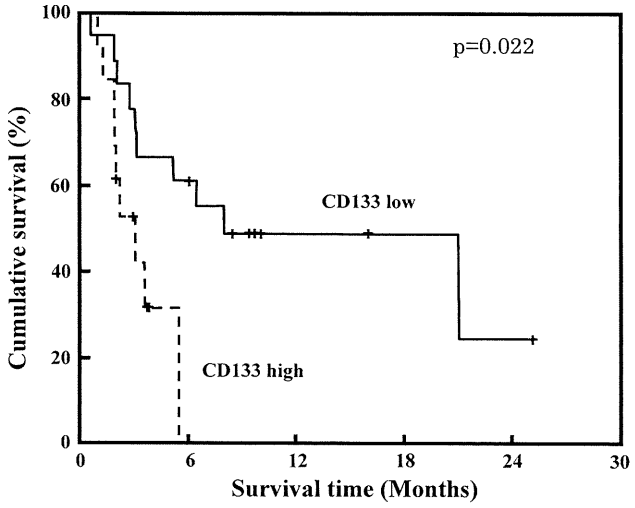

Fig. 5 Kaplan–Meier curve of overall survival in patients treated with combination therapy of S-1 and PEG-IFN α-2b, stratified according to the CD133 expression level

Toxicity

NCI-CTC grade 3 leukocytopenia, neutropenia, anemia, and thrombocytopenia were observed in 2 (6%), 2 (6%), 1 (3%), and 3 (10%) of the 31 patients, respectively. Grade 3 anorexia, stomatitis, rash, and fatigue were observed in 1 (3%), 1 (3%), 1 (3%), and 2 (6%) of the 31 patients, respectively. All adverse effects were alleviated when the treatment was discontinued, leading to no cases of mortality.

Discussion

Here we sought to identify factors predicting the therapeutic effect of S1+ PEG-IFN α-2b therapy in patients with advanced HCC. We collected pathological samples of HCC from all registered patients and studied proteins considered to be related to the therapeutic effect. The expression level of CD133 was significantly correlated with the therapeutic effect, but the expression levels of TS, DPD, and IFNR2, and the presence or absence of p53 mutations were not.

CD133 is a glycoprotein with five transmembrane regions and is a known blood stem-cell marker [28]. It also reportedly acts as a leukemia [15], brain [16], and colon cancer [17, 18] stem-cell marker. The characteristics of cancer stem cells include an ability to proliferate (self-replication capacity) and to differentiate into several cell types with different functions (multidifferentiation capacity), as well as a tumorigenic capacity, which was verified as tumor reproducibility in an experiment involving tumor implantation in an animal model [29–31]. In HCC, CD133-positive cells reportedly possess each of these cancer stem-cell characteristics. In 2007, Ma et al. [32] showed that 65–95% of cells in multiple HCC cell lines were CD133-positive, and Suetsugu et al. [33] reported that the HCC cell line Huh7 expressed CD133. In addition, Song et al. [34], who evaluated 60 patients with HCC, reported both significantly longer postoperative recurrence-free survival and total survival periods in a group with a low compared to that with a high CD133 level. There have been a few such reports on CD133 as a marker of postoperative recurrence.

In the present study, the CD133 protein expression level was significantly lower in the responder group than that in the nonresponder group. HCC showing high-level CD133 expression was resistant to the combination therapy used in this study. Several studies have suggested that the most cancer stem cells exist in the G_0 phase, and a reduced cell cycle velocity is involved in the drug resistance of cancer stem cells [35]. Furthermore, these cells are resistant to reactive oxygen-induced DNA damage because of their high radical-scavenging activities [36]. Furthermore, the drug resistance mechanism of cancer stem cells may also involve ATP binding cassette (ABC) transporters [16, 37]. The anti-apoptotic factors Akt/PKB and Bcl-2 are also activated in CD133-positive liver cancer cells by 5FU administration [38]. Because the anticancer effect of S1+ PEG-IFN α-2b therapy is primarily derived from apoptosis, the activation of Akt/PKB and Bcl-2 is considered to be directly related to the resistance to this therapy.

TS is a rate-regulating enzyme involved in the synthesis of deoxythymidine monophosphate, which is indispensable for DNA synthesis. Therefore, the anticancer effect of 5FU decreases when the TS expression level in the tumor is high, because the drug cannot sufficiently inhibit the enzyme [39]. In the present study, the TS expression level did not correlate with the therapeutic effect. Oie et al. [40] reported that TS expression was suppressed by IFN administration in all the HCC-derived cell lines they examined. Although we did not evaluate the TS expression level after IFN administration, the absence of a correlation between the TS expression level and the therapeutic effect may have been due to the inhibition of TS by IFN.

DPD is a 5FU-degrading enzyme present primarily in the liver. 5FU efficiency increases with low DPD expression in tumor cells [41]. In our study, no correlation between the DPD expression level and therapeutic effect was noted. This was an expected result, because S1 contains a DPD inhibitor.

IFNR, and particularly IFNR2, is considered to be the most important IFN-binding unit for IFN activity. IFNR2 is reportedly expressed in 61–77% of HCCs [42, 43], and its anticancer effect increases with its level of expression. In our study, IFNR2 expression did not correlate with the therapeutic effect. When multiple HCC cell lines were

treated with IFN-α in vitro, a relationship between IFNR2 expression and the anticancer effect was demonstrated [23]. Therefore, IFNR2 is undoubtedly important in the direct anticancer effect of IFN. However, indirect anticancer effects of IFN, such as the activation of natural killer cells and cytotoxic lymphocytes, must also be considered in regard to in vivo treatment [44–46]. Such indirect actions may be primarily responsible for the anticancer effects of IFN in some patients. Regardless of these findings, the IFNR2 expression level is not considered useful for the prediction of the therapeutic effect.

p53 is a typical tumor suppressor gene that may arrest the cell cycle and induce DNA repair or promote apoptosis, depending on the degree of DNA damage [47]. However, the mutation of p53 at some sites causes loss of its original function, allowing the initiation of tumor growth and acceleration of tumor proliferation [48]. In our study, no correlation was noted between the presence or absence of p53 mutations and the therapeutic effect. This may have been because there were only three patients with mutant p53, or because the mutations occurred at sites that do not affect p53 function.

In conclusion, S1+ PEG-IFN α-2b therapy can be a second-line treatment option for patients with advanced HCC, especially in those that show low CD133 expression. Further evaluation with a prospective randomized trial is necessary to confirm the results of the present study.

Acknowledgments The protocol of this study was approved by the Medical Committee of Kinki University of Medicine.

Conflict of interest None.

References

1. Kobayashi M, Ikeda K, Hosaka T, Sezaki H, Someya T, Akuta N, et al. Natural history of compensated cirrhosis in the Child–Pugh class A compared between 490 patients with hepatitis C and 167 with B virus infections. J Med Virol. 2006;78:459–65.
2. Okuda K, Fujimoto I, Hanai A, Urano Y. Changing incidence of hepatocellular carcinoma in Japan. Cancer Res. 1987;47: 4967–72.
3. Parkin DM, Bray F, Ferlay J, Pisani P. Global cancer statistics, 2002. CA Cancer J Clin. 2005;55:74–108.
4. Poon RT, Fan ST, Lo CM, Liu CL, Wong J. Intrahepatic recurrence after curative resection of hepatocellular carcinoma: long-term results of treatment and prognostic factors. Ann Surg. 1999;229:216–22.
5. Sato M, Watanabe Y, Ueda S, Iseki S, Abe Y, Sato N, et al. Microwave coagulation therapy for hepatocellular carcinoma. Gastroenterology. 1996;110:1507–14.
6. Yamasaki T, Kurokawa F, Shirahashi H, Kusano N, Hironaka K, Okita K. Percutaneous radiofrequency ablation therapy with combined angiography and computed tomography assistance for patients with hepatocellular carcinoma. Cancer. 2001;91:1342–8.
7. Llovet JM, Ricci S, Mazzaferro V, Hilgard P, Gane E, Blanc JF, et al. Sorafenib in advanced hepatocellular carcinoma. N Engl J Med. 2008;359:378–90.
8. Shirasaka T, Nakano K, Takechi T, Satake H, Uchida J, Fujioka A, et al. Antitumor activity of 1 M tegafur-0.4M 5-chloro-2, 4-dihydroxypyridine-1M potassium oxonate (S-1) against human colon carcinoma orthotopically implanted into nude rats. Cancer Res. 1996;56:2602–6.
9. Fukushima M, Satake H, Uchida J, Shimamoto Y, Kato T, Takechi T, et al. Preclinical antitumor efficacy of S-1; a new oral formulation of 5-fluorouracil on human tumor xenografts. Int J Oncol. 1998;13:693–8.
10. Cao S, Lu K, Tóth K, Slocum HK, Shirasaka T, Rustum YM. Persistent induction of apoptosis and suppression of mitosis as the basis for curative therapy with S-1, an oral 5-fluorouracil prodrug in a colorectal tumor model. Clin Cancer Res. 1999;5:267–74.
11. Sakon M, Nagano H, Dono K, Nakamori S, Umeshita K, Yamada A, et al. Combined intraarterial 5-fluorouracil and subcutaneous interferon-alpha therapy for advanced hepatocellular carcinoma with tumor thrombi in the major portal branches. Cancer. 2002;94:435–42.
12. Nakamura M, Nagano H, Marubashi S, Miyamoto A, Takeda Y, Kobayashi S, et al. Pilot study of combination chemotherapy of S-1, a novel oral DPD inhibitor, and interferon-alpha for advanced hepatocellular carcinoma with extrahepatic metastasis. Cancer. 2008;112:1765–71.
13. Ueshima K, Kudo M, Nagai T, Tatsumi C, Ueda T, Takahashi S, et al. Combination therapy with S-1 and pegylated interferon alpha for advanced hepatocellular carcinoma. Oncology. 2008;75:106–13.
14. Uka K, Aikata H, Mori N, Takaki S, Kawakami Y, Azakami T, et al. Combination therapy of oral fluoropyrimidine anticancer drug S-1 and interferon alpha for HCC patients with extrahepatic metastasis. Oncology. 2008;75:8–16.
15. Lapidot T, Sirard C, Vormoor J, Murdoch B, Hoang T, Caceres-Cortes J, et al. A cell initiating human acute myeloid leukaemia after transplantation into SCID mice. Nature. 1994;367:645–8.
16. Singh SK, Hawkins C, Clarke ID, Squire JA, Bayani J, Hide T, et al. Identification of human brain tumour initiating cells. Nature. 2004;432:396–401.
17. O'Brien CA, Pollett A, Gallinger S, Dick JE. A human colon cancer cell capable of initiating tumour growth in immunodeficient mice. Nature. 2007;445:106–10.
18. Ricci-Vitiani L, Lombardi DG, Pilozzi E, Biffoni M, Todaro M, Peschle C, et al. Identification and expansion of human colon-cancer-initiating cells. Nature. 2007;445:111–5.
19. O'Brien SG, Guilhot F, Larson RA, Gathmann I, Baccarani M, Cervantes F, et al. Imatinib compared with interferon and low-dose cytarabine for newly diagnosed chronic-phase chronic myeloid leukemia. N Engl J Med. 2003;13:994–1004.
20. Yasui K, Mihara S, Zhao C, Okamoto H, Saito-Ohara F, Tomida A, et al. Alteration in copy numbers of genes as a mechanism for acquired drug resistance. Cancer Res. 2004;64:1403–10.
21. Shintani Y, Ohta M, Hirabayashi H, Tanaka H, Iuchi K, Nakagawa K, et al. New prognostic indicator for non-small-cell lung cancer, quantitation of thymidylate synthase by real-time reverse transcription polymerase chain reaction. Int J Cancer. 2003;104:790–5.
22. Mcleod HL, Sludden J, Murray GI, Keenan RA, Davidson AI, Park K, et al. Characterization of dihydropyrimidine dehydrogenase in human colorectal tumors. Br J Cancer. 1998;77:461–5.
23. Yano H, Iemura A, Haramaki M, Ogasawara S, Takayama A, Akiba J, et al. Interferon alfa receptor expression and growth inhibition by interferon alfa in human liver cancer cell lines. Hepatology. 1999;29:1708–17.